Bioprinting and plastic compression of large pigmented and vascularized human dermo-epidermal skin substitutes by means of a new robotic platform

Luca Pontiggia[1,4]* iD, Ingmar AJ Van Hengel[1]*,**, Agnes S Klar[1,4], Dominic Rütsche[1,4], Monica Nanni[1,4,7], Andreas Scheidegger[5], Sandro Figi[5], Ernst Reichmann[1,4], Ueli Moehrlen[1,2,3,4,6] and Thomas Biedermann[1,4]

Abstract

Extensive availability of engineered autologous dermo-epidermal skin substitutes (DESS) with functional and structural properties of normal human skin represents a goal for the treatment of large skin defects such as severe burns. Recently, a clinical phase I trial with this type of DESS was successfully completed, which included patients own keratinocytes and fibroblasts. Yet, two important features of natural skin were missing: pigmentation and vascularization. The first has important physiological and psychological implications for the patient, the second impacts survival and quality of the graft. Additionally, accurate reproduction of large amounts of patient's skin in an automated way is essential for upscaling DESS production. Therefore, in the present study, we implemented a new robotic unit (called SkinFactory) for 3D bioprinting of pigmented and pre-vascularized DESS using normal human skin derived fibroblasts, blood- and lymphatic endothelial cells, keratinocytes, and melanocytes. We show the feasibility of our approach by demonstrating the viability of all the cells after printing in vitro, the integrity of the reconstituted capillary network in vivo after transplantation to immunodeficient rats and the anastomosis to the vascular plexus of the host. Our work has to be considered as a proof of concept in view of the implementation of an extended platform, which fully automatize the process of skin substitution: this would be a considerable improvement of the treatment of burn victims and patients with severe skin lesions based on patients own skin derived cells.

[1]Tissue Biology Research Unit, Department of Pediatric Surgery, University Children's Hospital Zurich, University of Zurich, Zurich, Switzerland
[2]Department of Pediatric Surgery, University Children's Hospital Zurich, University of Zurich, Zurich, Switzerland
[3]Zurich Center for Fetal Diagnosis and Treatment, Zurich, Switzerland
[4]Children's Research Center, University Children's Hospital Zurich, Zurich, Switzerland
[5]regenHU Ltd, Villaz-St-Pierre, Switzerland
[6]University of Zurich, Zurich, Switzerland
[7]Institute for Mechanical Systems, Department of Mechanical and Process Engineering, ETH Zurich, Zurich, Switzerland

*These authors contributed equally to this work and are considered to be co-first authors.
**New address: Department of Biomechanical Engineering, Delft University of Technology, Delft, The Netherlands.

Corresponding author:
Luca Pontiggia, Department of Surgery, Tissue Biology Research Unit, University Children's Hospital Zurich, Wagistrasse 12, Schlieren CH-8952, Switzerland.
Email: luca.pontiggia@kispi.uzh.ch
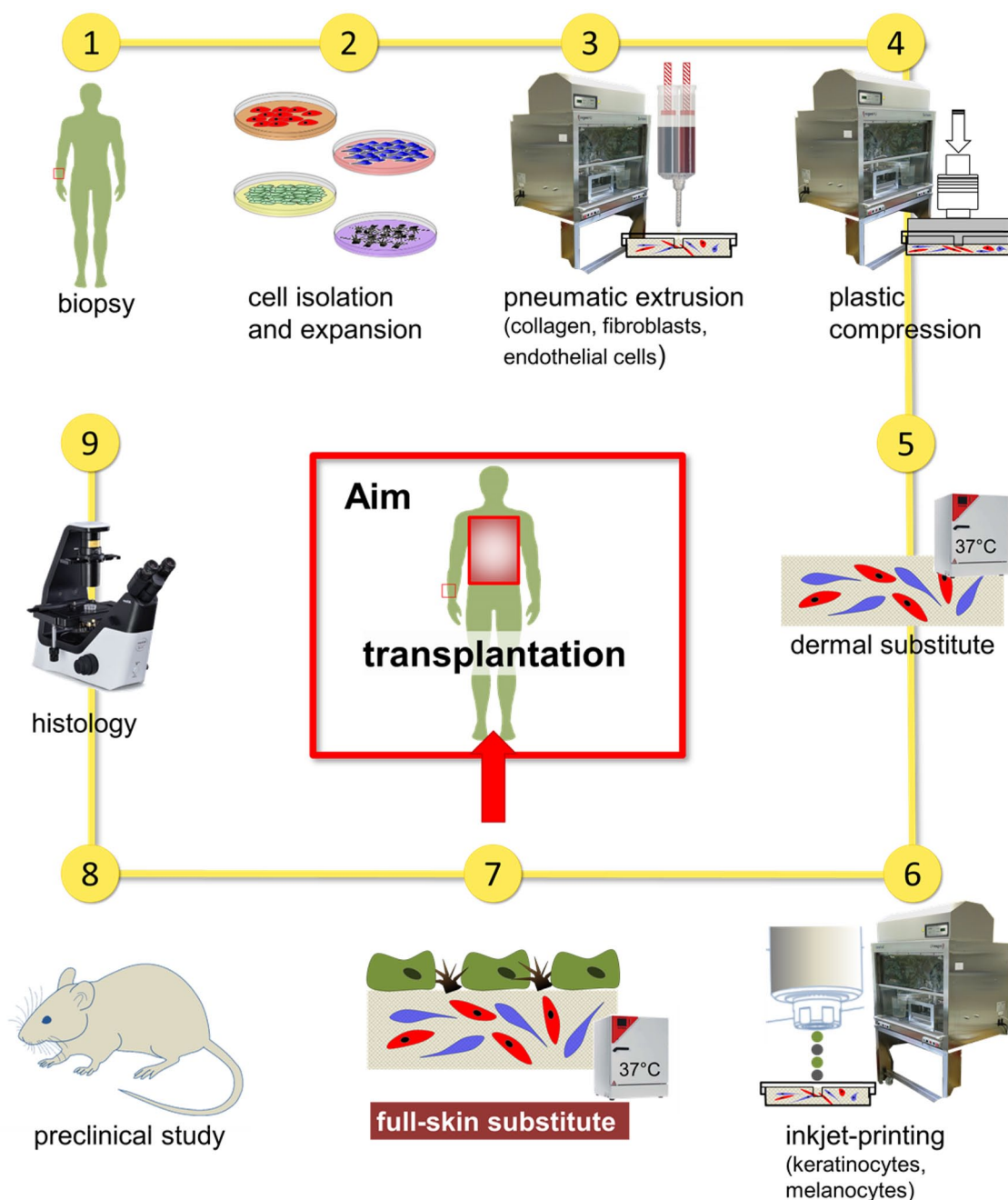
Graphical Abstract. The SkinFactory: Bioprinting and plastic compression of large pigmented and vascularized human dermo-epidermal skin substitutes.

Introduction

Split-thickness skin autografts (STS) still represent the gold standard to treat full thickness skin wounds. Thereby, part of the healthy skin is removed from a donor site on the patient's body and transplanted onto the wound area.[1,2] Unfortunately, the availability of autografts for wound coverage is insufficient when dealing with large and/or severe wounds. In addition, due to scar tissue development and contraction of the transplanted skin, this procedure often needs to be repeated to allow joint movement and body growth. This results in recurring painful treatments and long hospitalization periods for the patient.[3,4]

Therefore, great efforts regarding the development of skin substitutes were made in the last decades to overcome problems associated with STS including skin donor site shortage and scar formation.[5] Some examples are cultured epidermal autografts (CEAs), like EpiCell®, EpiDex®, and MySkin® that replace missing epidermis, and acellular dermal substitutes like Matriderm® and Integra® that are applied to prepare a neodermis.[3,6,7] Dermal substitutes are sometimes combined with CEAs, or keratinocytes sprays like ReCell® and

CryoSkin®, in a single or in two operative steps to cover deep wounds in a sort of dermo-epidermal composite. Furthermore, allogenic dermo-epidermal skin analogs including Apligraf® are used only for temporary cover of chronic wounds.[3,6,7] In contrast, dermo-epidermal skin substitutes (DESS) with autologous keratinocytes and fibroblasts represent a promising novel treatment option, however they are produced for compassionate use, not for commercialization.[8–12]

Therefore, the creation of an ideal tissue-engineered autologous dermo-epidermal skin substitute with functional and structural properties of normal human skin as a commercially available products to be available for patients all around the world is envisioned.[13] So far, preclinical studies with manually prepared skin grafts based on collagen type I matrix containing human fibroblasts as dermal part and a multi-layered epidermis consisting of keratinocytes were performed.[14–21]

Recently, we successfully performed and concluded a clinical application in a phase I trial, which demonstrated that these autologous dermo-epidermal skin equivalents developed in a safe and stable tissue, with nearly normal skin quality.[22]

In addition, Gómez et al.[23] successfully used a bioengineered skin composite for the clinical treatment of burn patients, using autologous fibroblasts and keratinocytes and clotted human plasma as a three-dimensional dermal scaffold.

Although considerable progress has been made, some important functional properties of skin, like pigmentation and vascularization, are still missing in the DESS. Despite the pivotal role of pigmentation in the protection of epidermal cells from ultraviolet radiation, the loss of homogeneous, natural pigmentation in skin substitutes also substantially affects the psychological and social well-being of the patients.[12,24–26] It was observed that a minimal number of melanocytes is necessary to obtain a homogeneous pigmentation matching the color of the donor skin in pigmented DESS.[18,24] In addition, the use of melanocytes resulted in a physiological response to UV-radiation in the pigmented DESS.[27] Importantly, mesenchymal cells influence melanosome production, maturation in melanocytes, and melanin transfer to keratinocytes, emphasizing the importance of using donor site-specific stromal cells in pigmented DESS, when aiming to produce skin grafts matching the color of the site to be transplanted.[28]

Next to pigmentation, the inclusion of a functional vascular network in the DESS in order to accelerate the connection with the host blood and nutrients supply was investigated: Endothelial cells from different origin (human umbilical vein, human dermis, or adipose tissue) could be induced to form a vascular plexus in fibrin hydrogels, collagen-based hydrogels, or scaffold-free substitutes.[14,20,29] With human dermal microvascular endothelial cells (HDMECs), lymphatic capillaries were successfully engineered, improving

cellular waste/debris removal, thus, reducing edema upon transplantation of DESS onto immunodeficient rats.[30]

Furthermore, an important feature of our DESS assembly approach is the plastic compression of the collagen type I used as matrix for the dermal part in the DESS. Thereby, the plastic compression mechanically stabilizes the dermal component of the DESS. Autologous human fibroblasts can be evenly distributed in the three dimensions of the hydrogel and can be plastically compressed without affecting their viability and biological function.[31] However, the combination of pre-vascularization and pigmented plastically compressed collagen-based DESS has never been shown before.

Further, accurate production of a large quantity of DESS in an automated way is an important goal for the treatment of severe large skin defects. To achieve this goal, 3D bioprinting is considered as a powerful tool. Hence, different technologies have been tested in the past with extrusion, jetting, and laser-based bioprinting being the most common.[32–34] Extrusion bioprinting consists in the dispersion of a bioink through a micro-nozzle using pneumatic pressure or a piston.[35] The extrusion printing allows to easily dispense highly viscous (bio-)materials, like soluble collagen, and is thus the gentlest method with respect to the viability of the cells. Jetting-based bioprinting with single droplet deposition utilizes either vibrating piezoelectric crystals, heating, or electrostatic forces to generate inkjets, which drives materials (cells) out of the nozzle toward the substrates.[36] Even though the print heads tend to clog frequently, the viability of the cells is well preserved. Laser-based bioprinting is a relatively complex technique, which uses pulsed laser energy to produce high-pressure blisters on a gold-coated tape. The burst of the blister directs the bioink to the substrate. Laser-based bioprinting is a nozzle-free procedure, which does not have clogging problems with cells or materials as for example jetting-based bioprinting, but shows a lower cell viability in comparison to the other techniques.[37] The combination of all of these different technologies, in particular extrusion and jetting-based bioprinting, enables the use of several bioinks such as polymerizing and jellifying materials, like fibrin and collagen, soluble factors, and living cells in a very specific and precise pattern, thereby eminently qualifying 3D bioprinting for skin analog production.[38–40]

Here, we describe our newly developed 3D bio-printer platform, which includes modules for collagen type I hydrogel mixing and extrusion-based bioprinting, hydrogel compression, and patterned inkjet delivery of various human skin derived cells. By means of this new robotic unit (called SkinFactory), we engineered for the first time a large-scale human DESS, which includes at the same time human skin derived keratinocytes, melanocytes, fibroblasts, and blood and lymphatic endothelial cells forming blood and lymphatic networks in vitro. Additionally, we demonstrate the functionality of the human pigmented and pre-vascularized DESS both in vitro and in a pre-clinical animal model in vivo.

Our work should be considered as a proof of concept in view of the implementation of a robotic platform, which would eventually fully automatize the entire manufacturing process of skin substitutes under GMP conditions for improved treatment of patients with severe skin lesions.

Materials and methods

Cell isolation and culture

Human foreskin and adipose tissue samples were obtained from the Department of Surgery of the University Children's Hospital Zurich. Parents or patients gave informed consent. This study was conducted according to the Declaration of Helsinki Principles and after permission by the Ethics Commission of the Canton Zurich (BASEC No. 2018-00269).

Human epidermal keratinocytes, melanocytes, dermal fibroblasts, and human dermal microvascular endothelial cells (HDMECs) were isolated from foreskin and cultured according to previously published routine protocols: Keratinocytes and fibroblasts according to Pontiggia et al.,[41] melanocytes as described in Böttcher-Haberzeth et al.,[21] HDMECs according to Montaño et al.[14] All isolation procedures are summarized in the supplemental protocols.

Preparation of dermo-epidermal skin substitutes without a bio-printer

This paragraph describes the non-automated preparation of DESS; the automated process is illustrated in Section 2.3. For this, collagen type I (5 mg/ml, Symathèse, Chaponost, France) hydrogels were prepared based on a previously published protocol[31] with some modifications. We used a newly developed transwell system (see also Section 2.3.2) consisting of 6×6 cm cell culture insert with a bottom PET track etched membrane with 3.0 μm pore size (custom made by Oxyphen, Wetzikon, Switzerland) placed in a 150 cm² cell culture flask with re-closable lid (TPP, Trasadingen, Switzerland). Six millilitres neutralization buffer (0.32 M NaHCO$_3$, 0.15 M NaOH, 200 mM Hepes, Sigma-Aldrich Chemie GmbH, Buchs, Switzerland), 4 ml Dulbecco's modified Eagle's medium (DMEM, Gibco, Thermo Fisher Scientific AG, Basel, Switzerland) containing 0.4×10^6 fibroblasts and 30 ml collagen were mixed and poured into the cell culture insert. After 1 h of incubation at 37°C the hydrogel was compressed to the thickness of 1 mm (final cell concentration: 120 cell/mm³) and incubated for 1 week at 37°C in 40 ml DMEM (supplemented with 10% Fetal Calf Serum, 0.05% Gentamycin, and 1% Hepes Buffer 1 M, all Thermo Fisher) in the lower chamber of the transwell system and 10 ml in the upper chamber of the insert. Medium was changed three times a week.

After 1 week, keratinocytes and melanocytes were mixed in proportion 5:1 in serum-free keratinocytes medium (SFM, supplemented with 25 mg/ml bovine pituitary extract, 0.2 ng/ml EGF, and 5 mg/ml gentamycin; all Thermo Fisher) and melanocytes growth medium (MGM, PromoCell, Heidelberg, Germany), also in a 5:1 ratio (SFM:MGM). The ratio of about one melanocyte to five keratinocytes was taken in accordance with the described findings about the physiological distribution of melanocytes in the basal layer of the human epidermis.[28,42] 0.45×10^6 cells were seeded on the top of the hydrogel. The skin substitutes, now called DESS, were incubated at 37°C in DMEM with 40 ml of medium in the lower chamber only, to avoid the flushing of seeded keratinocytes and melanocytes on the surface of the hydrogel. The next day, 10 ml of SFM:MGM, were gently added onto the epidermal part of the DESS. The culture media were changed three times a week. After 1 week of incubation, fluorescein diacetate (FdA, Sigma-Aldrich) live cell staining was performed to verify cell viability.

For the pre-vascularization of DESS, HDMECs were mixed with fibroblasts in a ratio of 1:1 (8.2×10^5/ml) and included in the hydrogel which was then cultured in EGM-2MV medium (Lonza, Basel, Switzerland) for 3 weeks before receiving keratinocytes and melanocytes in the same way as described above. Then, DESS were cultured with 40 ml EGM in the lower and 10 ml SFM:MGM in the upper chamber. The culture media were changed three times a week. After 1 week of incubation, fluorescein diacetate (FdA, Sigma-Aldrich) live cell staining was performed to verify cell viability.

All the steps of the procedure, the used media and the culture times are summarized in Table 1.

The 3D bio-printer SkinFactory and the automatized generation of DESS

To engineer pigmented and vascularized DESS according to the protocol above, we used the BioFactory™ 3D bio-printer system of regenHU (Villaz-Saint-Pierre, Switzerland). The BioFactory™ was supplemented with automated hydrogel-mixing/extrusion, compression, and jetting devices to create a robotic platform with four different stations applied to a turning turret, like a carrousel. The modified version of the BioFactory™ was called "SkinFactory." Figure 1 schematically describes the different components of the SkinFactory and the custom-made consumables (schematics in b, c, d by RegenHU with Autodesk Inventor (Autodesk, San Rafael, USA), drawing in e by Oxyphen AG with 3D CAD (Autodesk)). Figure 2 shows photographs of the skin producing process. In the following section, we describe in detail the SkinFactory operative procedures, which implements the protocol (concentrations, media) as, described in Section 2.2.

Step I: Bioink and cartridge preparation. The cartridge (Medmix, Rotkreuz, Switzerland) for the bioink consisted of a double syringe with two separate compartments (Figure 1(a),

**Table 1.** Summary of the used cells, media, and culture times.
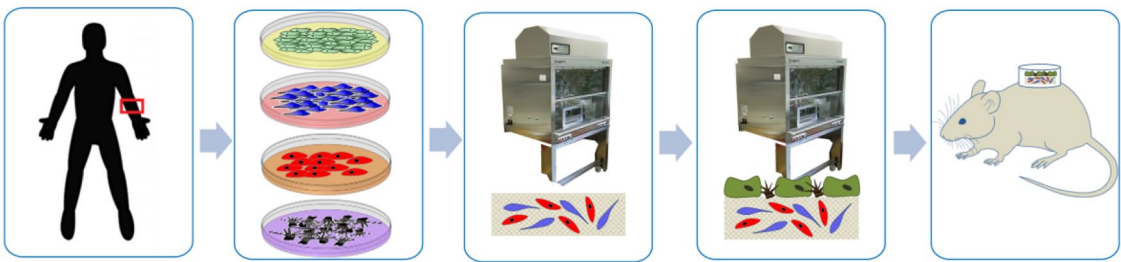
Procedure step	Biopsy	Cell isolation and culture	Dermis formation and hydrogel compression	Cell printing of epidermal compartment	Transplantation
Pigmented DESS	Day 0	Day 1–14	Day 7	Day 14	Day 21
	Foreskin • Dermis • Epidermis	Fibroblasts Keratinocytes Melanocytes	Collagen Fibroblasts	Keratinocytes Melanocytes	Onto full-thickness skin lesion nu/nu rats
Used media		DMEM SFM MGM	DMEM	SFM:MGM 5:1 (top) DMEM (bottom)	
Prevascularized DESS with HDMECs	Day 0	Day 1–28	Day 14	Day 28	Day 35
	Foreskin • Dermis • Epidermis	HDMECs Fibroblasts Keratinocytes Melanocytes	Collagen HDMECs Fibroblasts	Keratinocytes Melanocytes	Onto full-thickness skin lesion nu/nu rats
Used media		EGM DMEM SFM MGM	EGM	SFM:MGM 5:1 (top) EGM (bottom)	
Number of cells (number of possible hydrogels)	Day 0 3–5 cm^2	Day 1 K: 6–10 $\times$ 10^6 E: 0.1–0.2 $\times$ 10^6 F: 0.5–1.5 $\times$ 10^6 M: 0.1–0.2 $\times$ 10^6	Day 7 E: ~0.8 $\times$ 10^6 (4) F: ~3 $\times$ 10^6 (15)	Day 14 K: ~25 $\times$ 10^6 (60) M: ~1 $\times$ 10^6 (13)	

DMEM: Dulbecco's modified Eagle's medium; E: endothelial cells; EGM: endothelial cell growth medium; F: fibroblasts; HDMECs: human dermal microvascular endothelial cells; K: keratinocytes; M: melanocytes; MGM: melanocyte growth medium; SFM: serum free medium for keratinocytes.

Crt). The ratio between the volumes of the compartments was 2:1. For filling, the cartridge was closed with a cap (Ca). One component of the bioink, consisting of the fibroblasts/ endothelial cells suspension, was poured into the small compartment of the cartridge and mixed with the neutralization buffer. The other component of the bioink, collagen type I, was cast into the large compartment. Then, both syringes were sealed with O-ring pistons (Ps). Next, the cartridge was turned up site down and the cap (Ca) was substituted with the mixer (Mx). The bioink filled cartridge (Figure 1(a), to the right) was then loaded into the SkinFactory.

Step II: Preparation of the dermal equivalent using the SkinFactory. Figures 1(b), 2(b) and (c) show the first station of the turning turret. The loaded cartridge was inserted into the cartridge holder (Ch). The 6 × 6 cm (internal size) cell culture insert (In, also in Figure 1(c) and (e)) was placed on the

stage (St). The insert was held in position by the insert holder (Ih, Figure 2(c)). During the two-component mixing and deposing process, the insert bottom was positioned exactly 3.3 cm under the opening of the mixer. The plungers (pl) pushed the content of the two compartments through the mixer opening (4 mm) into the insert (Figures 1(b) and 2(c)) at a flow rate of 0.8 ml/s (dosing resolution: 2.9033 µl/ step; cartridge piston surface: 580.66 mm^2 × 0.005 mm minimal axis resolution; shear rate approx. 130 s^{-1}). The measured viscosity of the bioink (collagen type I and neutralized cell suspension) was 0.166 Pa s (Supplemental Figure S1a). During extrusion the stage performed circular movements to allow an homogeneous distribution of a single layer of the bioink on the porous membrane, resulting in a 6 × 6 cm hydrogel (dermal equivalent) with 8 mm of thickness. During the jellification of the collagen a storage modulus of approximately G′ = 200 Pa was reached after
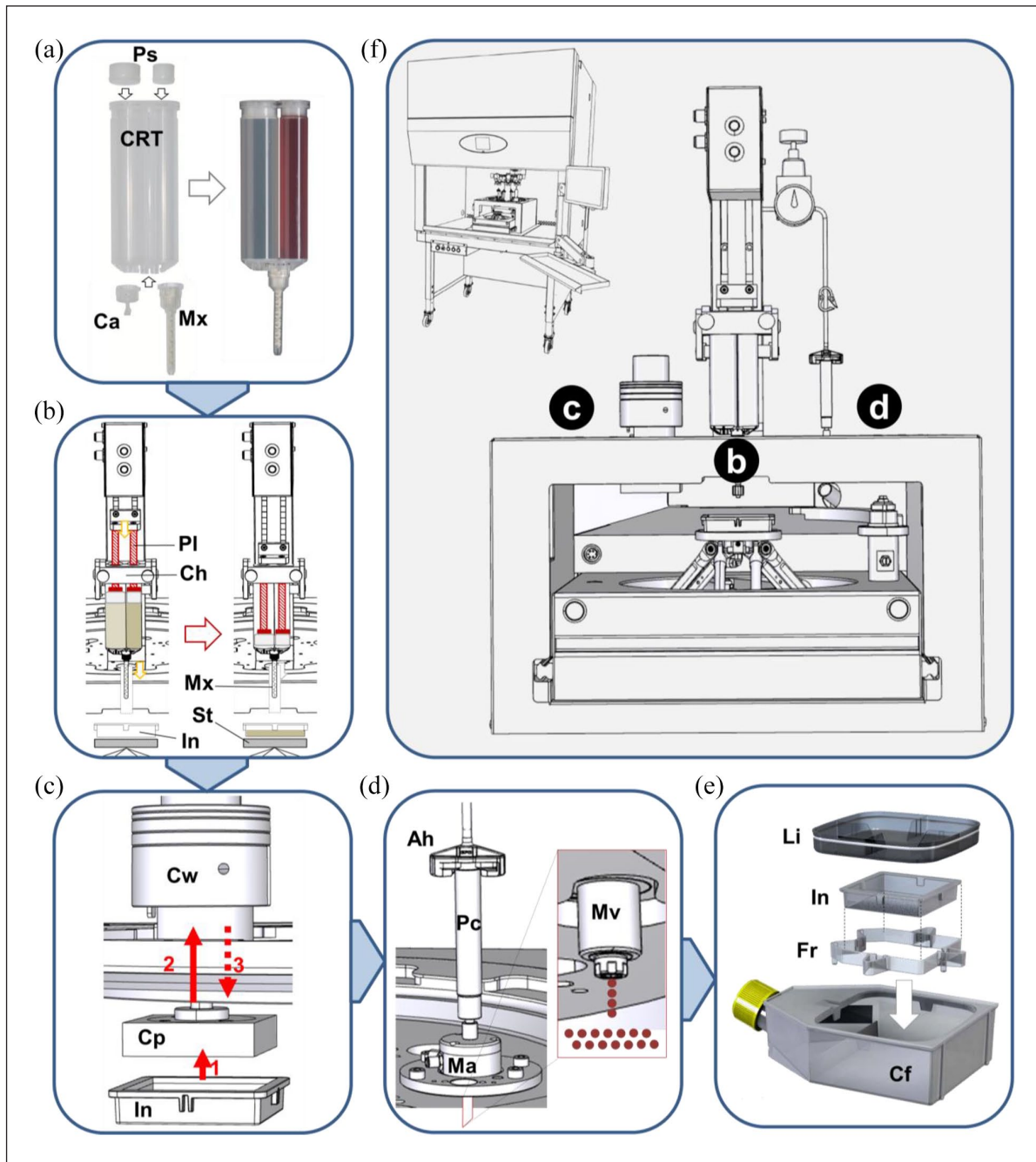
Figure 1. Schematic illustration of the robotic platform SkinFactory. (a) Loading of the cartridge with collagen type I and human dermal cells. (b) Production of the dermal component by pressure assisted extrusion. (c) Hydrogel plastic compression. (d) Inkjet-based bioprinting of human epidermal cells. (e) Cell culture system. (f) Overview of the turning SkinFactory platform. Station b: pressure assisted extrusion, station c: plastic compression, station d: Inkjet-bioprinting.

Ah: cartridge adapter head; Ca: cap; Cf: cell culture flask; Ch: cartridge holder; Cp: compression piston; Crt: cartridge; Cw: compression weights; Fr: insert frame; In: culture insert; Li: culture flask lid; Ma: microvalve actuator; Mv: microvalve; Mx: mixer; Pl: plunger; Ps: o-ring pistons; Pv: pressure valve; St: stage.

1 h, the loss modulus only rose to $G'' = 14$ Pa, indicating the formation of a solid hydrogel (Supplemental Figure S1b).

Step III: Plastic compression of the dermal component using the SkinFactory. For compression, the turret of the SkinFactory was turned to the second station. The white square compression piston (Figure 1(c), Cp) of the compression device was now just above the insert (In). For compression, the stage was moved slowly up until the piston was in contact with the hydrogel (red arrow 1 and Figure 2(d)). The movement upward continued for the thickness of the uncompressed hydrogel (Hg in Figure 2(d), approximately
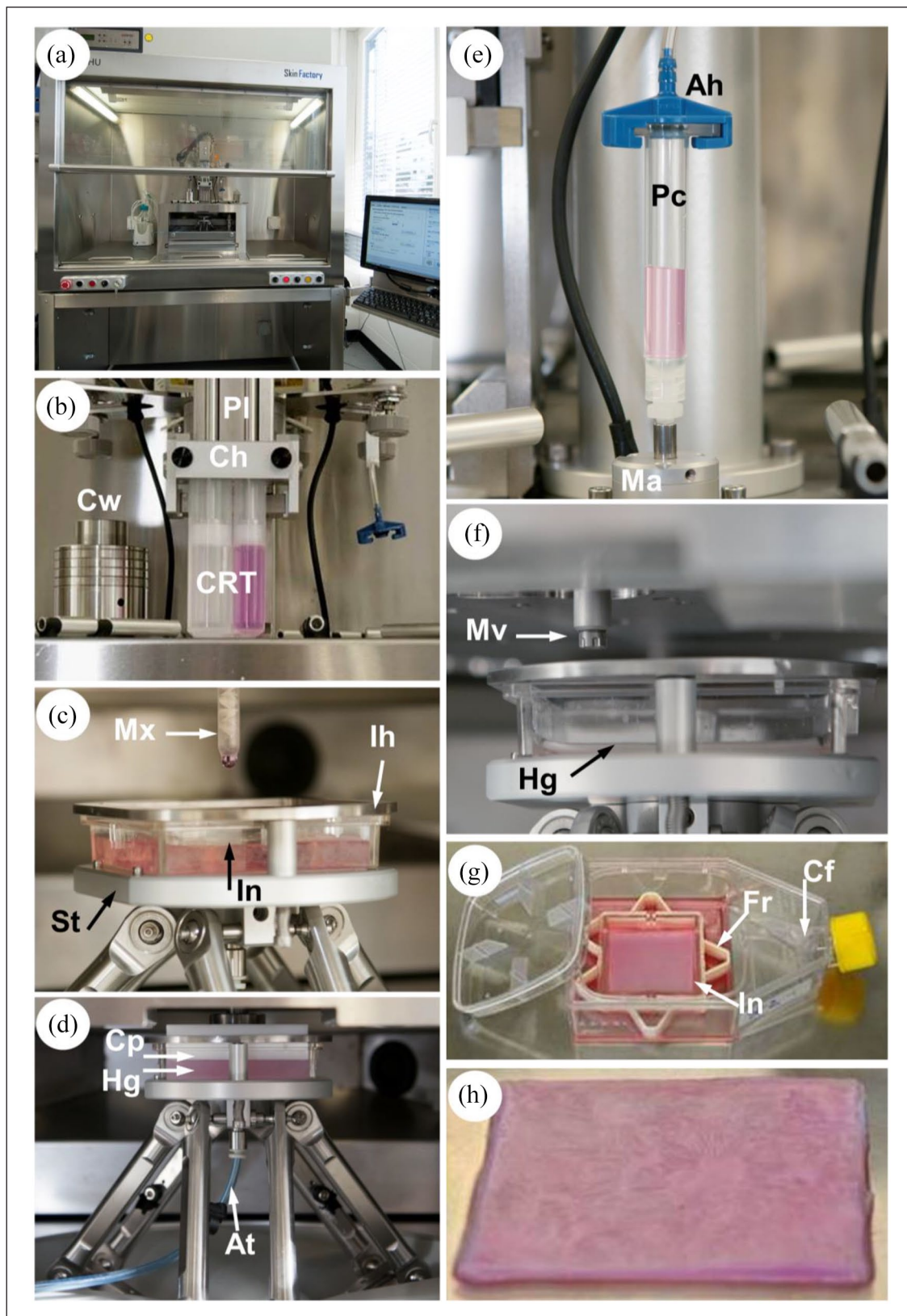
Figure 2. Skin substitute production process. (a) Front view of the SkinFactory. (b) Production of the dermal component by pressure assisted extrusion. (d) Hydrogel plastic compression. (e) Inkjet-based bioprinting of human epidermal cells. (g) Cell culture system. (h) Pre-vascularized pigmented human dermo-epidermal skin substitute of $6 \times 6\,cm^2$. Abbreviations as for Figure 1.
At: aspiration tube; Hg: hydrogel; Ih: insert holder.

0.8 cm) *minus* the desired final thickness of the compressed hydrogel, which was 1 mm (red arrow 2). During this second movement, the compression weights (Cw) were pushed upward. Gravitation generated a compression force of 600g to the hydrogel (red dotted arrow 3). Fluid (cell culture medium) was pushed out through the porous membrane of the insert into a blotting paper and was removed by aspiration through a tube (At) connected to the bottom of the stage (Figure 2(d)). Thereafter the culture insert containing the hydrogel was removed from the SkinFactory stage, inserted in a frame (Fr, Figure 1(e)), and transferred into a 150 cm^2 cell culture flask (Cf) with reclosable lid containing the appropriate medium. The compressive (Young's) modulus of the plastically compressed collagen hydrogels was measured as 27.12 ± 5.22 kPa (n = 3, see supplemental protocols). Other structural parameters of the obtained hydrogels where analyzed in previous publications.[31,43]

Step IV: Printing of the epidermis using the SkinFactory. The cell suspension of keratinocytes and melanocytes was loaded into the printing cartridge (Pc, Figures 1(d) and 2(e)) which was sealed by the cartridge adapter head (Ah). The head was connected to a compressed air system delivering a pressure of 0.1 bar (Pv). The tip of the cartridge was connected through a lure lock adapter to the microvalve actuator (Ma). A microvalve (Mv, opening diameter 100 μm) regulated the dispensed volume by the frequency of openings (shots, Figures 1(d) and 2(f)). For this study, droplets consisting of two shots of 0.4 μl were printed. This resulted in 0.8 μl dots with a diameter of 1.9–2.5 mm. The number of cells contained in the droplet was regulated by means of the cell concentration in the used cell suspension. We defined for this study 4000 cells/dot. Around 109 dots (0.436 Mio cells) were evenly distributed on the 36 cm^2 surface of the hydrogel (compare Figure 3) by the movement of the stage, resulting finally in a DESS. A software interface (BioCAD™, regenHU) facilitated the drawing of the printing pattern.

Step V: Culturing of the skin substitute. After printing of keratinocytes and melanocytes, the culture insert containing the DESS was removed from the SkinFactory stage, inserted in a frame (Fr, Figure 1(e)), and transferred into the 150 cm^2 cell culture flask (Cf) with reclosable lid containing the EGM medium (Figure 2(g)). No medium was added in the insert (upper chamber) to avoid the flushing of printed keratinocytes and melanocytes on the surface of the hydrogel. The frame maintained the insert 5 mm above the bottom. The next day, 10 ml of SFM:MGM, was gently added on top of the insert. After 1 week incubation at 37°C/5% CO$_2$, FdA live cell staining was performed to verify cell viability. DESS was now ready for transplantation (Figure 2(h)). Figures 1(f) and 2(a) are overviews of the SkinFactory platform.

Animals and transplantation

Animal studies were approved by the local committee for experimental animal research (license number ZH90/15)

and performed as previously published.[15] The surgical protocol was approved by the local Committee for Experimental Animal Research (permission number: ZH090/2015). Ten weeks old immune-incompetent female crl:NIH-Foxn1rnu rats (Charles River, Freiburg, Germany) were prepared and anesthetized as described previously.[44,45] Skin substitutes were transplanted into full thickness skin defects created surgically on the back of the animals. To prevent wound closure from rat skin, custom made metal rings (2.5 cm in diameter) were sutured to the skin defects using non-absorbable polyester sutures (Ethicon, Johnson and Johnson, Zug, Switzerland). Buprenorphin (s.c. 0.05 mg/kg body weight, Temgesic™, Indivior AG, Baar, Switzerland) was applied for analgesia. Dressing changes and photographic pictures were made once a week. After 3 weeks, transplants were excised and embedded either in paraffin or TissueTek (OCT compound, Sakura, Alphen aan den Rijn, Netherlands) for histological and immunofluorescence analysis.

Histological, fluorescence, and live cell staining

Fluorescein diacetate (FdA) live cell staining was performed according to the protocol previously published.[31] Histological hematoxylin/eosin and immunofluorescence staining on tissue sections were described in detail by Biedermann et al.[15] and whole mount staining by Marino et al.[30] All the used antibodies were specific for human antigens if not differently specified: from Abcam (Cambridge, UK): Lyve1 (polyclonal, 1:100, ab10278); from BD Pharmingen (Basel, Switzerland): Ki67 (clone: B56, 1:100); from Dako: human CD31 (clone: JC70A, 1:50), rat CD31 (clone: TLD-3A12, 1:50), CK10 (clone: DE-K10, 1:100), Melanosome (HMB45, 1:50); from Dianova (Germany): CD90 (clone: AS02, 1:50); from Lubio (Luzern, Switzerland): CK1 (clone: LHK1, 1:200); from Progen (Heidelberg, Germany): CK5 (polyclonal, 1:100, GP-CK5); from SantaCruz (Labforce AG, Nunningen, Switzerland): Laminin 332 (clone: P3H9-2, 1:100), Tyrosinase (clone: c-19, 1:50), VE-Cadherin (clone: F-8, 1:50); from Spring Bioscience (CA, Pleasanton): CK15 (clone: SPM190, 1:50). The counterstaining of cell nuclei was performed with Hoechst 33342 (Sigma-Aldrich). Pictures were taken with a DS-Ri1 digital camera connected to a Nikon Eclipse TE2000-U inverted microscope. The device is equipped with Hoechst-, FITC-, and TRITC-filter sets (Nikon AG, Switzerland; Software: NIS-Elements BR version 3.22.11).

Cell quantification

Transplanted DESS were stained for Ki67 and imaged with the 20x objective. The ratio of proliferative nuclei (Ki67 positive) over total nuclei (Hoechst positive) in five representative photographic frames each (n = 5) were quantified. In the same way, HMB45 positive melanocytes over DAPI positive nuclei were quantified.
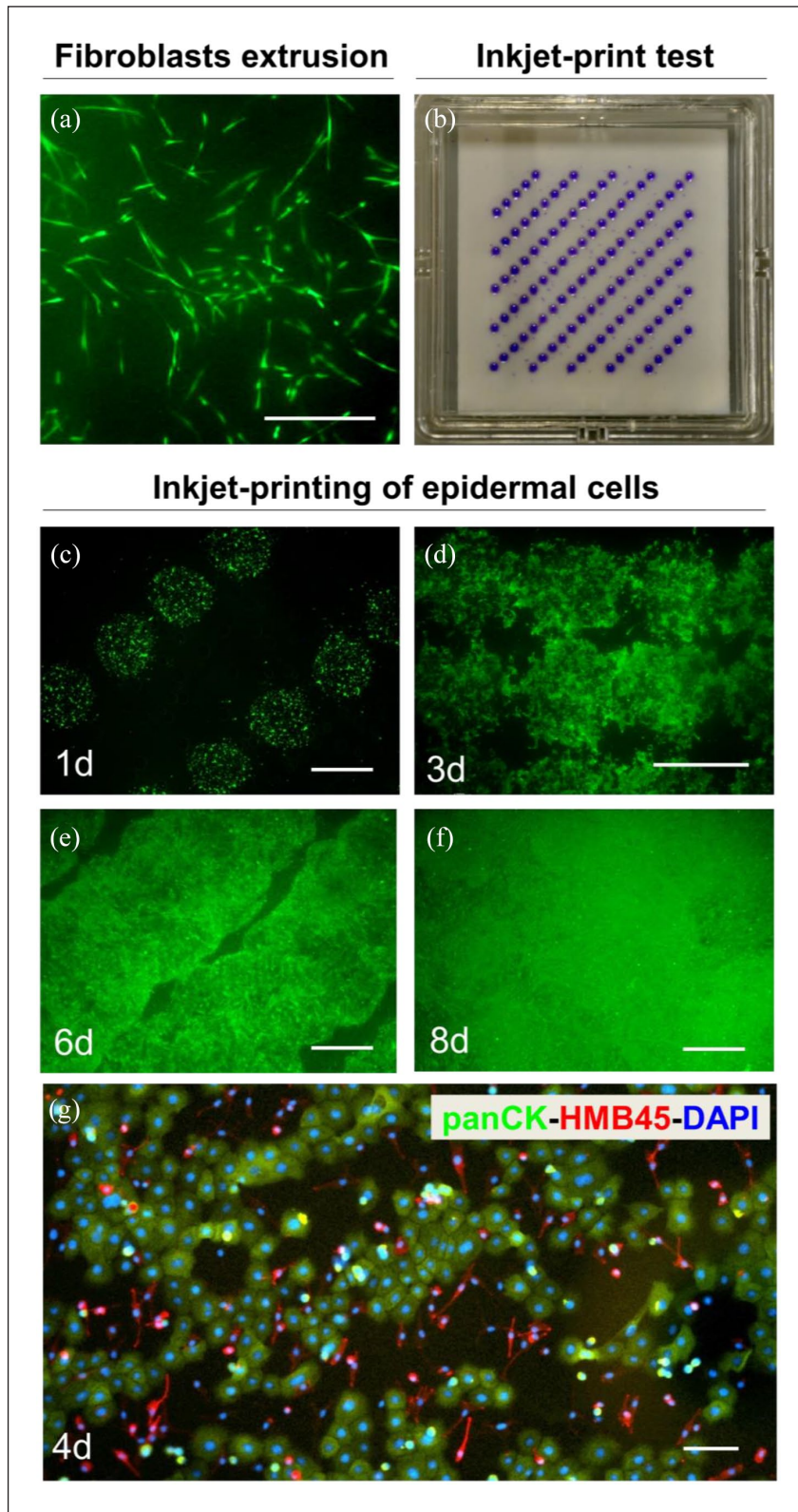
Figure 3. Patterned cell printing resulted in a coherent layer of human keratinocytes and melanocytes. (a) FdA staining of human fibroblasts in a collagen type I hydrogel 7 days after hydrogel production. (b) The programed printing pattern for keratinocyte and melanocyte seeding was visualized by printing of trypan blue on a filter paper. (c–f) Inkjet-based bioprinting of epidermal cells: FdA staining of keratinocytes and melanocytes 1 day (c), 3 days (d), 6 days (e), and 8 days (f) after printing. (g) Immunofluorescence staining of cells 4 days after seeding with antibodies against panCK (keratinocytes, green) and HMB45 (melanocytes, red). Counterstaining of cell nuclei with Hoechst (blue). Scale bars: 100 μm in (a); 2 mm in (c–f).

All results are reported as mean ± standard error of the mean (±SEM). Comparison between two groups was performed using the unpaired Student's *t* test. Differences were considered significant with a $p < 0.05$.

Results

For the transition from our established manual production of dermo-epidermal skin substitutes (DESS) to automated assembly of pigmented and vascularized DESS using the SkinFactory, we investigated several points including (i) the homogeneity of the cell distribution in the different compartments, namely epidermis and dermis, (ii) the survival of the cells during the different printing steps, and (iii) cell viability and functionality in the substitutes in vitro and in vivo after transplantation.

Dermal fibroblasts tolerate the collagen extrusion and compression process, and patterned jet-printing is safe for epidermal keratinocytes/melanocytes

The two basic steps of the DESS assembly consist of (i) the inclusion of dermal cells in collagen to form the dermal component and (ii) the printing of the epidermal cells to create the epidermal compartment of the skin equivalent.

Thus, we first investigated the homogeneity of distribution of fibroblasts only, included in the collagen matrix by the automated extrusion process and analyzed the viability of the fibroblasts after the mixing procedure. We used the SkinFactory to embed fibroblasts in the collagen type I matrix and to compress the created dermal substitute. After 1 week of culture, we evaluated the viability and distribution of the dermal cells by FdA staining. Figure 3(a) shows a representative sector of a compressed bioprinted collagen hydrogel, where the fibroblasts displayed their characteristic elongated shape, and populated homogeneously the collagen matrix. This fibroblast pattern in the automated process was comparable to the manually prepared collagen matrix (data not shown) and was thus considered a prerequisite for the decision to proceed with the generation of an epidermal layer.

We asked further, how dense keratinocytes and melanocytes have to be printed on top of the bioprinted hydrogel to form a homogenous closed layer and how viable are the cells after the jetting process. For this, we first optimized the jetting pattern for the total size of the hydrogel (6×6 cm), and figured out that 109 droplets were the optimal number for our jetting conditions: the minimal number of droplets and consequently the minimal number of cells which allows the coverage of the whole surface of the hydrogel in a period of time of no more than 1 week. For better visualization of the printing pattern, trypan blue droplets were jet-printed directly on the porous membrane of the insert (Figure 3(b)).

Accordingly, 7 days after formation of the dermal component (Figure 3(a)), keratinocytes and melanocytes were mixed in a 5:1 ratio and printed in 109 dots with 4000 cells each on the 6×6 cm collagen hydrogel. Repetitive FdA cell staining revealed that the epidermal cells well-tolerated the jetting pressure, were viable, migrated and formed a coherent layer within 8 days after printing (Figures 3(c)–(f), 1, 3, 6, and 8 days). During this time, at day 4, we performed immunofluorescence staining using panCK (green) and HMB45 (red) antibodies. The first antibody react against several cytokeratins and the second against a neuraminidase-sensitive sialylated glycoconjugate present in pre- and earlystage melanosomes. They are useful for the identification of keratinocytes and melanocytes, respectively (Figure 3(g)). Both cell types were present and uniformly distributed on the collagen type I hydrogel. Melanocytes displayed their characteristic elongated structure with some protrusions and keratinocytes showed a typical cobblestone pattern.

Pigmented bio-printed dermo-epidermal skin substitutes are functional in vivo

Following the verification of cell viability after the bioprinting process in vitro, we investigated whether the bioprinted melanocytes were able to sustain pigmentation of DESS in vivo.

Bio-printed human DESS containing fibroblasts, keratinocytes, and melanocytes were transplanted onto the back of immuno-incompetent female nu/nu rats 7 days after seeding of the epithelial cells. Three weeks after transplantation, the DESS showed macroscopically a slight pigmentation (Figure 4(a)). Histological analysis of frozen sections revealed the presence of all the strata of the epidermis, including the stratum basale (Figure 4(b), white arrows), stratum spinosum (black star), and stratum corneum (white box). Melanin was visible after Fontana Masson staining (Figure 4(c), black arrows), and further, melanin was deposited above the nuclei of keratinocytes (blue arrows). Immunofluorescence analysis showed the presence of melanocytes in the basal layer by expression of tyrosinase, an enzyme that catalyzes the *production* of *melanin* (Figure 4(d)), and the melanosome-marker PMEL (HMB45, Figure 4(e)).

The expression of laminin 332 (the ligand of keratinocyte integrin α6β4 in hemidesmosomes), was indicative for a homogeneous basement membrane (Figure 4(e)). To determine the proliferative capacity of the epithelial cells in the DESS, sections were stained for Ki67, a nuclear cell proliferation-associated antigen that is expressed in all active stages of the cell cycle[46] (Figure 4(f)). The basal keratinocyte layer homogeneously expressed cytokeratin (CK) 15 (Figure 4(g)) and CK5 (Figure 4(h)). CK15 is a
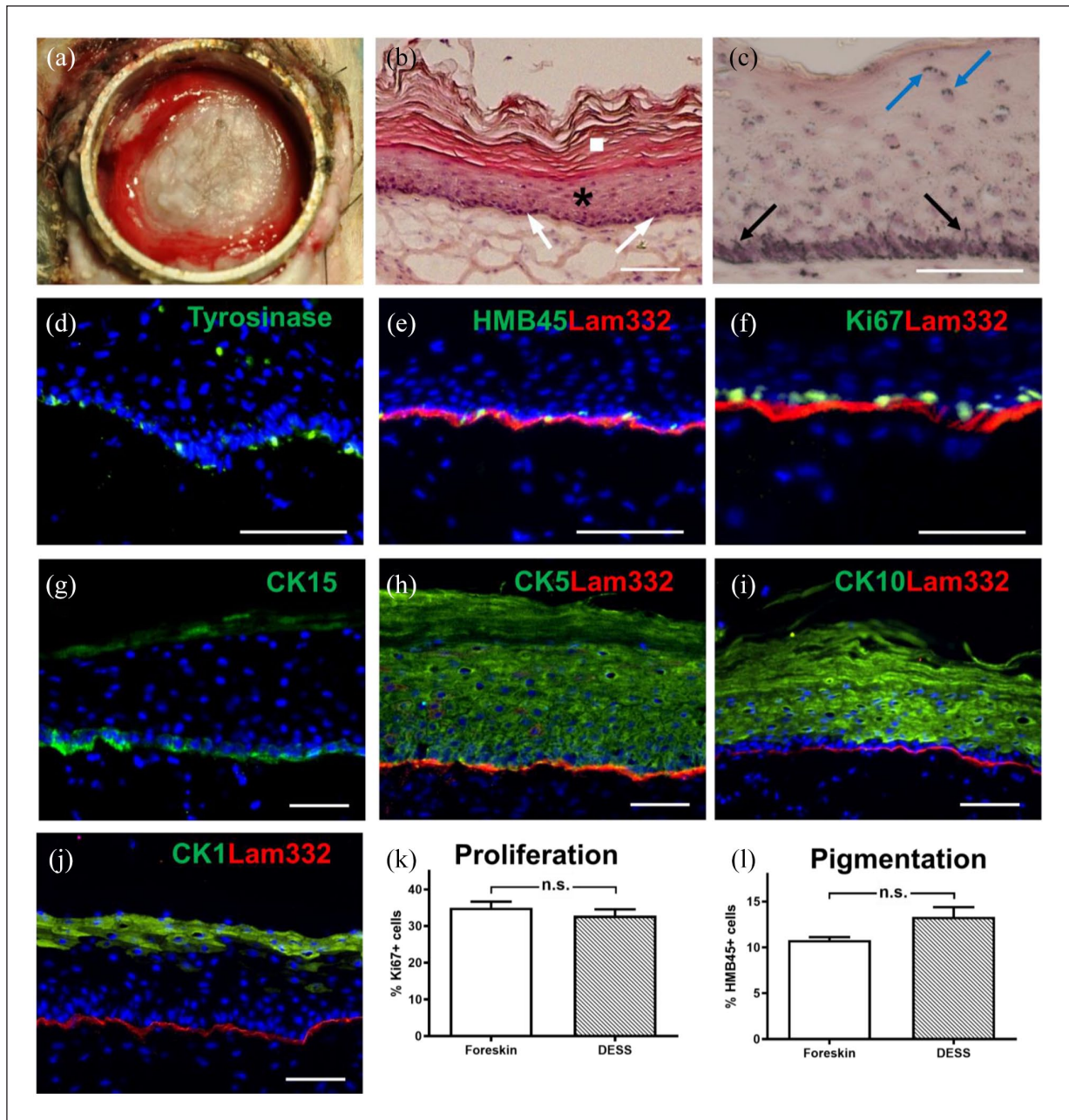
Figure 4. Analysis of a pigmented human DESS in vivo. (a) Macroscopic view of the human graft 3 weeks after transplantation. (b) Hematoxylin/eosin staining of sections showing the stratum basale (arrows), stratum spinosum and stratum granulosum (star), and stratum corneum (square). (c) Fontana-Masson melanin staining. Cell nuclei and cytoplasm were counterstained with Hematoxylin/eosin. Melanocyte dendrites projecting to the upper layers of the epidermis (black arrows) and melanosomes shielding keratinocytes nuclei (blue arrows) are visible. (d–j) Immunofluorescence staining using antibodies to: Tyrosinase ((d), green), HMB45 (green)/Lam332 (red) (e), Ki67 (green)/Lam332 (red) (f), CK15 ((g), green), CK5 (green)/Lam332 (red) (h), CK10 (green)/Lam322 (red) (i), CK1 (green)/Lam332 (red) (j). Counterstaining of cell nuclei with Hoechst (blue). (k) Quantification (n = 5) of proliferating cells (Ki67^{+}) in DESS and in foreskin as a control. (l) Quantification (n = 5) of melanocytes (HMB45^{+}) in DESS and in foreskin as a control. Results are reported as mean ± standard error of the mean (±SEM). Comparison between two groups was performed using the unpaired Student's *t* test. Differences were considered significant with a $p < 0.05$. Scale bars: 100 μm.

useful indicator of epidermal homeostasis, as it is almost exclusively expressed in basal keratinocytes in a homeostatic epidermis.[41] In normal human homeostatic epidermis, CK5 is expressed in the basal layer and the first suprabasal layers. However, expression of CK5 is induced in activated keratinocytes during wound regeneration.[15] The CK5 expression pattern shows that after 3 weeks the graft in our system has not yet reached homeostasis.
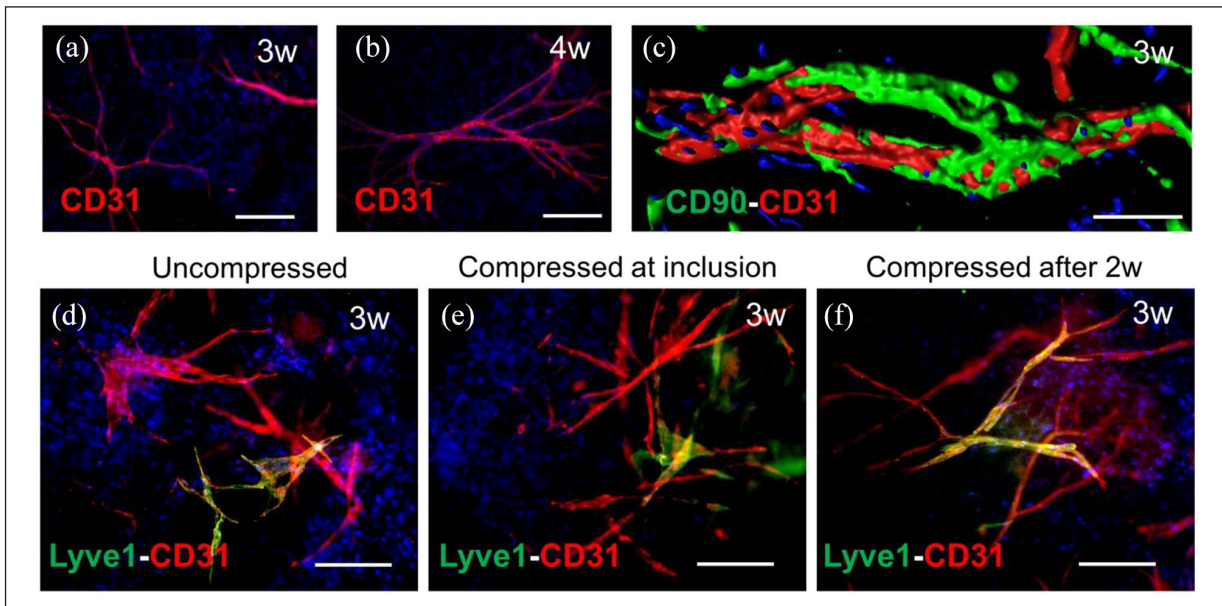
Figure 5. SkinFactory production of pre-vascularized human DESS in vitro. (a) CD31 immunofluorescence whole-mount staining showing the formation of capillaries from HDMECs in collagen type I hydrogels upon 3 weeks and (b) 4 weeks of culture after SkinFactory production. (c) CD31/CD90 double staining and confocal imaging with volume reconstruction of HDMECs-derived capillaries upon 3 weeks of culture in a collagen type I hydrogel displaying the presence of mural cells (CD90 positive) around endothelial cells (CD31 positive). (d–f) CD31 (red)/Lyve1 (green) immunofluorescence staining of HDMECs (BECs and LECs) raised in collagen hydrogels for 3 weeks under three different conditions: uncompressed (d), compressed upon HDMECs inclusion (e), or compressed 2 weeks after inclusion (f). Counterstaining of cell nuclei with Hoechst (blue). In all three cases lymphatic (yellow CD31/lyve1 double positive) and blood capillaries (red CD31 single positive) were visible. Scale bars are 100 μm.

The differentiation marker CK10 (Figure 4(i)) was expressed in the suprabasal layers of the spinous and granular layers, whereas CK1, a late differentiation marker, was still confined to the stratum granulosum (Figure 4(j)). Both, the suprabasal expression of CK5 and the missing expression of CK1 in the spinous layer may indicate that the graft did not reach complete homeostasis after 3 weeks in vivo. The percentage of Ki67-positive proliferative cells (32.83% $\pm$ 1.7%, mean $\pm$ SEM; Figure 4(k)) was statistically similar compared to Ki67 expressing epidermal cells in foreskin used as control (35.0% $\pm$ 1.7%, p=0.51). HMB45-expressing melanocytes were visible in the basal layer at an occurrence similar to control human skin: 13.3% $\pm$ 1.1% HMB45-positive melanocytes in DESS versus 10.8% $\pm$ 0.32% (p=0.21) in foreskin (Figure 4(l)).

Automated mixing and compression of hydrogels allow pre-vascularization of dermal substitutes in vitro

After the engineering of pigmented DESS, we introduced a vascular network into the dermal compartment of the pigmented DESS.

To first investigate the influence of the SkinFactory on the vascular network formation, hydrogels were produced without compression and epidermal cells. For this,

HDMECs and fibroblasts were included into collagen type I hydrogels and plated in 6×6 cm inserts with the SkinFactory system. The hydrogels were not compressed with the SkinFactory and cultured up to 4 weeks in vitro. Subsequently, the hydrogels were analyzed by whole mount immunofluorescence staining after 3 and 4 weeks. Figure 5 shows the formation of branched capillaries after 3 and 4 weeks as judged by the CD31 expression in representative sectors of the hydrogels (Figure 5(a) and (b)). Confocal microscopy revealed the 3D vascular network and the partial coverage of the CD31 expressing capillaries by CD90 (Thy-1) positive mural cells (Figure 5(c)).

To elucidate the effect of plastic compression on the capillary formation in vitro, in particular to define the optimal time point, at which compression is best tolerated by the endothelial cells, HDMEC containing collagen hydrogels were produced and compressed using the SkinFactory just after production or 2 weeks later, when a capillary network was already present in the hydrogels.

In general, we observed the formation of capillary networks in all conditions (Figure 5). In uncompressed collagen hydrogels, serving as controls, HDMEC developed into blood and lymphatic capillaries within 3 weeks (Figure 5(d)). But even in both types of compressed hydrogels (Figure 5(e) and (f)), we could equally observe the formation of blood (positive for the pan endothelial marker CD31 only) or lymphatic capillaries (positive for CD31

and the lymphatic marker Lyve1), indicating that compression do not impair the formation of the vascular plexus.

Fully automated engineering and transplantation of pigmented and pre-vascularized dermo-epidermal skin substitutes (PV-DESS)

We finally combined pigmentation and pre-vascularization to assemble the first automatically engineered pigmented and pre-vascularized dermo-epidermal skin substitute "PV-DESS" using the SkinFactory.

Hence, we combined HDMECs and fibroblasts in the dermal compressed compartment and keratinocytes with melanocytes in the epidermal component of the PV-DESS using the SkinFactory. We studied the functionality of the obtained human PV-DESS at 1–3 weeks after transplantation in our animal model (Figure 6). First, we investigated the presence of the human capillary network after transplantation. The human capillaries were monitored by immuno-fluorescence staining using the human CD31 antibody in combination with the human fibroblast marker CD90 (Figure 6(a)). We detected human capillaries 1 and 2 weeks after transplantation in the human dermis (Figure 6(a), upper panels). Importantly, also after transplantation, we could reveal both blood and lymphatic capillaries by immunofluorescence double staining for human CD31 and human Lyve1 (Figure 6(a), lower panels).

To demonstrate the integrity of the capillary network we performed immunofluorescence stainings against VE-Cadherin, a component of intercellular junctions of endothelial cells. Supplemental Figure S2a shows the expression of human VE-Cadherin (green) in capillaries expressing CD31 (red). The panel a′ illustrates the magnification of the region in the white box of Figure 2(a), whereas panel a″ shows the separate green and red channels. On the same grafts sections, we performed stainings against human (red) and rat CD31 (green) to reveal whether bioengineered human capillaries had anastomosed to the vascular plexus of the host. Supplemental Figure S2b shows that the human capillaries, present in the bioengineered human dermis, connected to the host rat vessels: the white arrows indicate yellow anastomosis regions where both hCD31 and rCD31 molecules coexist spatially very tight together. Anastomosis of human and rat capillaries is also demonstrated by the presence of auto-fluorescent rat erythrocytes (green) in human capillaries (CD31 in red) (Supplemental Figure S2c). The arrowhead points at a CD31 negative rat vessel, whereas the arrow and Supplemental Figures S2c′ and c″ indicate a CD31 positive human vessel.

By means of hematoxylin/eosin staining, the upper panel of Figure 6(b) demonstrates the quality of the obtained PV-DESS 2 weeks after transplantation with a pronounced cornified layer (white star), an ordered

stratification (black star), and basal keratinocytes arranged as a typical columnar layer of cells (white arrowhead) interpolated with melanin containing melanocytes (black arrowheads), which extend their protrusions into the upper layer (arrows). To prove the presence and the localization of all used human cell types, a four-color immunofluorescence staining (Figure 6(b), lower panel) was performed to delineate fibroblasts (CD90, blue), endothelial cells (CD31, white), keratinocytes (CK1, red), and melanocytes (HMB45, green).

Further histological hematoxylin/eosin analysis showed a stratified epidermis (Figure 6(c), top panels) after 1, 2, and 3 weeks in vivo. A mature physiological keratinocyte pattern in the different layers and in particular in the basal layer was visible after 2 and 3 weeks, displaying columnar basal keratinocytes (white arrowhead). A cornified layer was hardly distinguished after two and clearly present after 3 weeks (white stars). CK10 was expressed from the first week on (Figure 6(c), second row), but was still observed in the basal layer (white arrowheads) of the epidermis after 1 week. However, after 2 weeks, CK10 was definitely confined to the suprabasal layers (white arrowheads), highlighting epidermal homeostasis. The Ki67 expression was mainly located in the basal layer (Figure 6(c), third row) after 1, 2, and 3 weeks. The analysis of proliferative cells in representative regions of transplanted PV-DESS confirmed $22\% \pm 4.8\%$ in the 3 weeks substitutes compared to $35\% \pm 1.7\%$ positive cells in normal human foreskin (Figure 6(d), mean $\pm$ SEM). This difference was calculated as not significant ($p=0.17$) so this result is not different from the result with the non vascularized subsites (Figure 4(k)). We observed that $13.3\% \pm 1.8\%$ cells in the basal layer of DESS are melanocytes (Figure 6(c), last row and Figure 6(e)), compared to $11\% \pm 0.3\%$ (n.s., $p=0.45$) basal layer melanocytes in normal human foreskin, demonstrating a physiological number of melanocytes in our PV-DESS.

Figure 6(f) shows the macroscopic view of a PV-DESS transplant 3 weeks after transplantation.

Discussion

The engineering of autologous dermo-epidermal skin substitutes (DESS) with the functional and structural properties of normal human skin represents encouraging treatment of large severe burns, trauma, congenital giant nevi, and diseases that lead to skin necrosis. In the last years, autologous dermo-epidermal skin analogs prepared in a manual manner were established[15,17,31,41] and preclinical long term transplantation experiments were performed.[15,18,19,21] This work resulted for example in a completed clinical phase I trial, which demonstrated that DESS are safe and result in stable tissues, with nearly normal skin quality.[22] The recently started multicentric phase II study will further prove the quality of these autologous
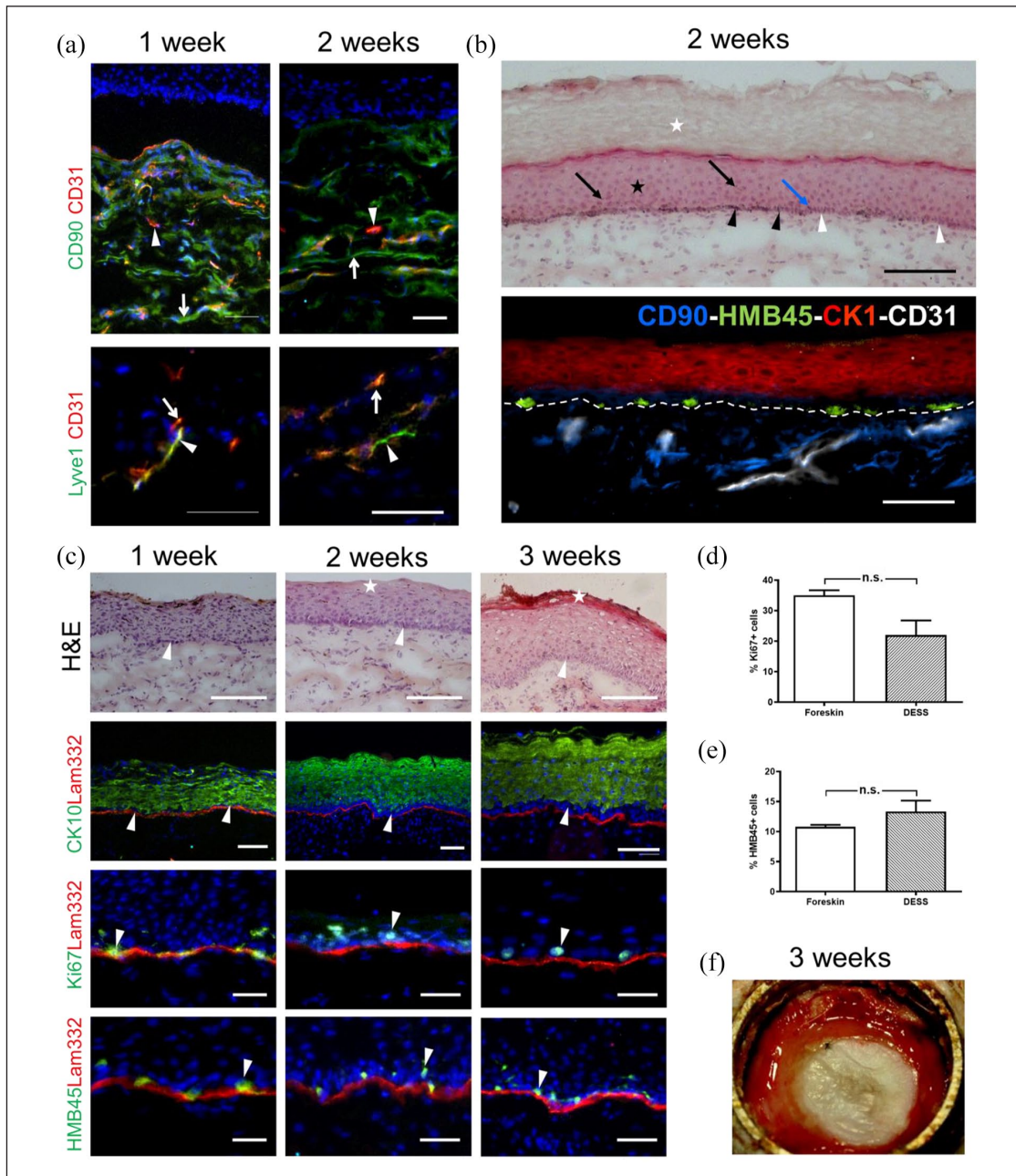
Figure 6. In vivo investigation of bio-printed pigmented and pre-vascularized human DESS using the SkinFactory. (a) Human capillaries (CD31, red, arrow heads) are present in the human neo-dermis, which is highlighted by human dermal fibroblasts (CD90, green, arrows), 1 and 2 weeks after transplantation (upper panels). Human Lyve1 (green) and human CD31 expression (red) demonstrate the presence of both lymphatic (arrow heads) and blood capillaries (arrows) 1 and 2 weeks after transplantation (lower panels). (b) Hematoxylin/eosin staining (upper panel): stratum corneum (white star), stratum spinosum (black star), pigmented clusters of melanocytes (black arrow heads), unpigmented clusters of basal keratinocytes (white arrow heads), melanocyte dendrites (blue arrow), and melanosome supranuclear caps in keratinocytes (black arrows). (b′) Four-color immunofluorescence staining demonstrating the presence and the localization of the four included cell types: fibroblasts (CD90, blue), endothelial cells (CD31, white), Keratinocytes (CK1, red), and melanocytes (HMB45, green). The white dotted line indicates the dermo-epidermal border. (c) Additional histological and immunofluorescence analysis. First row: Hematoxylin/eosin staining showing the formation of multi-layered epidermis, basal, and cornified layers are indicated by arrowheads and stars, respectively. Second row: CK10 (green)/Lam332 (red) immunofluorescence double staining with arrowheads indicating the basal layer. Third row: Ki67 (green)/Lam332 (red) double staining with arrowheads indicating the proliferative cells. Fourth row: HMB45 (green)/Lam332 (red) double staining with the arrowheads indicating the melanocytes. Counterstaining of cell nuclei with Hoechst (blue). (d) Quantification (n = 5) of proliferative basal cells (Ki67^{+}) in DESS 3 weeks after transplantation and comparison to foreskin. (e) Quantification (n = 5) of melanocytes (HMB45^{+}) in the basal layer of DESS 3 weeks upon transplantation compared to foreskin. Results are reported as mean ± standard error of the mean (±SEM). Comparison between two groups was performed using the unpaired Student's t test. Differences were considered significant with a $p < 0.05$. (f) Macroscopic view of a DESS 3 week after transplantation. Scale bars are 200 μm.

DESS. For a future development and improvement of such DESS, two challenges became relevant. The first issue is related to the reproduction of important physiological properties of the skin, which are missing in the current DESS, namely pigmentation and vascularization. The second challenge is the automated production of high numbers of large-size DESS, without the need for manual DESS preparation, for improved reproducibility.

Hence, the present study aimed at the automated engineering of pigmented and pre-vascularized DESS as a proof of concept in view of the realization of a robotic platform, which would fully automatize, under GMP conditions, the whole process of DESS production. The 3D-printing platform of regenHU offered the necessary technological instrumentation and flexibility to implement our manual protocols in an automated assembly system. The pre-existing platform consisted of a microvalve ink-jetting device suitable for printing cells,[47–52] for example keratinocytes and melanocytes. We modified the platform by the addition of two new modules for our specific needs to establish the SkinFactory: The first module is made up of a piston-driven extrusion tool, which utilizes a double syringe and a mixer tip for combining collagen and cells (fibroblasts). The second module consists in a hydrogel compression device, which allowed to modulate thickness and stiffness of the skin equivalent. The mobile stage of the regenHU platform was adapted to keep in place the 6×6 cm cell culture insert of a new type of transwell system, which was custom made by Oxyphen for our purposes. This transwell system was created to fit in a commercially available 150 cm^2 cell culture flask with reclosable lid.

Through the production of a large pigmented pre-vascularized human DESS using the automated SkinFactory, we could show for the first time that (1) both blood and lymphatic capillary formation is not impaired by collagen type I hydrogel plastic compression, (2) jet-printed keratinocytes and melanocytes in programed patterns remain viable and developed into a coherent cell layer, and therefore that (3) the automated inclusion of five human skin derived cell types (blood- and lymphatic endothelial cells, fibroblasts, keratinocytes, and melanocytes) in a DESS is feasible.

Our established SkinFactory platform is based on the pre-existing BioFactory system which was used before in different studies to improve bioinks and printing precision,[47,48] or for tissue engineering of cartilage,[50] bone,[49] and retina.[52] The bioprinting of pigmented human skin by means of another BioFactory-based system was shown by Ng et al.[51] through the use of inkjet-modules only: their dermal component consisted of multiple layers of collagen, polyvinylpyrrolidone (PVP), and fibroblasts. The collagen used by Ng et al.[51] was neutralized prior to printing to allow jellification, but was maintained at low temperatures to avoid the clogging of the jetting-nozzle. In contrast to our

work, no endothelial cells were included and 4 days after formation of the dermal component, keratinocytes and melanocytes, suspended separately in the same PVP/collagen-based bioink, were dispensed separately on the dermal equivalent. Ng et al. maintained their constructs up to 4 weeks in vitro under air-liquid interface. Even though they obtained indeed a homogeneous pigmentation, the stratification of the epidermis upon transplantation was incomplete and unordered. The above-described strategy used by Ng et al. presents in our opinion some unaddressed points, which are generally also not taken into account by others, and which we investigated in our study.

The first point is the scaffold used to reconstruct the dermal component of the skin substitute. Biomaterials traditionally used for the production of (bioprinted) human skin analogs like fibrin[53–55] or collagen[38] are actually naturally derived and easy to apply, yet they are hampered by some disadvantages, like the poor mechanical strength, the rapid biodegradation rate, and the difficult printability. Additionally, cellularized collagen hydrogels often contract considerably during the in vitro culture phase.[56,57] Therefore, new strategies have been developed to overcome these drawbacks: for example the modification of the mechanical properties of collagen through chemical and biophysical cross-linking techniques,[58,59] or the use of artificially synthesized polymers such as polyvinylpyrrolidone,[51] polyethylene glycol,[60] and many others.[61] Yet, with the application of plastic compression to collagen I,[62] we obtained and characterized[43] the most natural biomaterial for skin reconstruction in a mechanically stable form with reduced shrinkage properties, thereby avoiding complex synthesis procedures. It was previously demonstrated that autologous human fibroblasts can be evenly distributed in the three dimensions of a hydrogel and can be plastically compressed without affecting their viability and biological function.[31] With our study, we demonstrated for the first time the feasibility of plastic-compression of pre-vascularized collagen-based DESS.

A second issue we want to emphasize is the technologies utilized for the printing of collagen with fibroblasts as the dermal component on one site and keratinocytes and melanocytes as the epidermal layer to the other site. Collagen I is soluble in acidic conditions and is relatively viscous. The jellification process requires pH-neutralization, which is generally achieved before printing by addition of a neutralization buffer,[63] or afterwards by sodium bicarbonate nebulization.[38] The first method, that is *pre*-neutralization, necessitates a cooling system to slow down jellification until the collagen reaches the final position and form.[63] This applies to both extrusion and inkjet-bioprinting. With the second method, that is *post*-neutralization, the risk of clotting of the jetting-nozzle is reduced (although not eliminated), but the layer-by-layer printing with subsequent nebulization is mandatory, which in turn, reduces the printing speed.[38,60,63,64] In contrast to the

aforementioned methods, we used an *intra*-neutralization process. For this, we exploited a double-syringe with two separate compartments, one for the collagen and one for the cells and neutralization buffer, which are mixed during printing (i.e. intra-neutralization). This simplifies preparation and loading of the bioinks and the technical requirements of the printing system (no cooling is necessary). In addition for dermal substitutes produced in horizontal molds, the extrusion technology is simpler, faster, and cheaper compared to inkjet-bioprinting. Regarding the deposition of keratinocytes and melanocytes by ink-jet bioprinting, we want to annotate that the same can also be performed by simple extrusion bioprinting. Though, we wanted to exploit all the features of our platform in view of future applications. These may include not only the high throughput production of skin substitutes by extrusion of epidermal cells in a standardized way, but also a site-specific single-cell deposition and patterning to reproduce, for example pigmentation gradients. For the present work, we were particularly interested in using ink-jet bioprinting to produce single dots of keratinocytes and observe the migration of keratinocytes to cover the whole hydrogel surface in a sort of wound healing assay. Future developments will indicate which approach (extrusion or ink-jet) will be used for which application (clinical or basic research studies).

A third consideration regards the restoration of the patient's native skin color in a skin analog. It was shown that adding melanocytes to bioengineered dermo-epidermal skin analogs allows to obtain pigmented DESS with high affinity to donor skin.[18] In the present work, we reproduced those results with the new SkinFactory. Similarly, Ng et al. tried to mimic the keratinocytes–melanocytes distribution and ratio in the human epidermis by sequential printing of keratinocytes and melanocytes at predetermined positions. They achieved indeed a homogeneous pigmentation in vitro,[51] yet, in our opinion, this approach is unnecessarily complex since it requires the pre-definition of the keratinocytes and melanocytes printing pattern. It is also more time consuming due to the separate delivery of the two cell types. On the other hand, many different factors concur to create a physiological environment for the correct development of pigmentation. These factors are certainly related to the scaffold and the interplay of different cell types present in it, or to the growth factors present in the culture media as well as the culture protocols. However, most of these factors still remain to be determined. It is therefore conceivable that a slight shift of the balance between all the unknowns will affect the development of a correct pigmentation.[54,64]

A fourth point concerns the efficient vascularization of DESS. After transplantation, non-vascularized tissue-engineered skin grafts are initially entirely dependent on diffusion, which is slow and inefficient.[65] The delivery of oxygen, nutrients, and growth factors, is often inadequate

and results in scar-like dermal structures and tissue shrinkage. The application of pre-vascularized grafts, which rapidly anastomose, with the blood capillaries of the host upon transplantation has been shown to promote cell survival, differentiation, and physiological integration of the engineered tissue.[20,66] The recent advancements in the field of 3D bioprinting of vascularized tissues[67] include three approaches: (i) the bioprinting of scaffolds with vascular-like microchannels to be populated by endothelial cells before transplantation,[68] (ii) the pre-patterned printing of endothelial cells that form a vascular plexus which can anastomose with the host vascular system,[69–71] and (iii) the random 3D-printing of a endothelial cell containing matrix and spontaneous self-assembly of microvascular structures. While the first approach is suited for the reconstruction of larger vessels, the other two aim at the regeneration of capillary structures. We based our SkinFactory experiments according to the third approach, as it was already successfully proved that endothelial cells spontaneously assembled and formed a vascular plexus in vitro.[14,72,73] Indeed, many 3D bioprinting protocols also rely on the remarkable self-assembly property of endothelial cells, yet with two variants: (a) the printing of the dermal component (with fibroblasts and endothelial cells) and consecutive printing of the epidermal compartment, followed by direct transplantation with the assembly of the vascular structures occurring in vivo,[74] or (b) a short microvascular development-phase in vitro is interposed between dermal and epidermal printing.[63] For the formation of a vascular network in our substitutes, according to the second variant, we included an apparently long (2 weeks), but, in our opinion, necessary development-phase in vitro. It was previously demonstrated, that this time is crucial for the correct development of the DESS and is, at the same time, the phase during which fibroblasts remodel the collagen hydrogel, prepare the formation of a basal lamina and thus the anchorage of epithelial cells, and secrete growth factors to finally sustain epidermal regeneration.[17] In addition, during this phase, a ramified 3D vascular plexus forms. Indeed, the reduced (or missing) dermal-maturation time can be one of the reasons for reduced stratification and vascularization of grafts in vitro.[38,54]

A fifth important issue is the choice of the origin of endothelial cells. Different sources of endothelial cells are generally used for vascular tissue engineering,[7,75] yet 3D bioprinting attempts were done mainly with umbilical cord cells (HUVECs),[29,68,76–78] but also with cord blood cells,[63] HDMECs,[74] and induced pluripotent stem cells (iPSC).[79] Both HUVECs and cord blood cells are allogeneic to the patient and potentially immune-reactive. Furthermore, investigators using HUVECs reported reduced survival and impaired in vivo skin engraftment.[80] Moreover, the in vivo vasculogenic capacity of cord blood-derived cells declines rapidly with time during cell culture.[81] We believe that the ideal clinical approach to create a pre-vascularized

dermal equivalent should use autologous cells, derived from a single biopsy, and easily harvested from the patient with minimal donor-site morbidity. Therefore, HDMECs are the best option since they match to the above-mentioned profile. The advantage of using HDMECs is that they are gained from the same biopsy in the same workflow as the other needed cell types, that is, fibroblasts, keratinocytes, and melanocytes, thus simplifying the isolation procedures and reducing donor-site morbidity.

A further consideration concerns the exposition of the substitutes to the air-liquid interphase to induce differentiation of the epidermal layer, as indicated by some of the mentioned authors.[38,51,53,60,64] According to published works,[17,63] we believe that exposition to the air-liquid interphase is beneficial only for the stratification and maintenance of the substitutes in vitro. In case of transplantation this step can be skipped, since the stratification of the new epidermis is supported by the host.[22]

Another aspect is that natural human skin shows a characteristic undulating pattern of rete ridges and alternating dermal papillae to increase the surface area of the dermo-epidermal junction. This provides mechanical stiffness to the skin and extends the capillary-epidermal interface to improve nutrient supply to the avascular epidermis.[82] Due to the presence of CK19/CK15 expressing cells in the tips of the rete ridges,[41,83,84] the additional role as reservoir of epidermal stem cells has also been proposed.[85] We have clues that the presence of a vascular plexus might be pivotal in the spontaneous formation of rete ridges structures (unpublished results). Also Baltazar et al.[63] observed similar outcomes and related the spontaneous development of rete ridges with the presence of supporting pericytes in their skin substitutes. Despite the presence of fibroblasts, which were shown to take over the role of pericytes,[20] we did not observe any formation of rete ridges in this study. In this respect, interesting attempts to create de novo rete ridges have been recently shown using PDMS patterned substrates coated with collagen I and cultured with keratinocytes in vitro,[86] using three-dimensional electrospun microfabricated scaffolds seeded with keratinocytes[87] or using laser ablation to create rete ridges-like patterned dermal templates which were covered by keratinocyte sheets and transplanted on nude mice.[88] Hence, we could easily address with our SkinFactory the issue to include preformed "ridges" which cells can occupy by performing the collagen compression step using a modified compression piston with a rete ridge like patterned surface in the future.

The upgrade of DESS to full-skin substitutes by the inclusion of the hypodermal layer is a possible and reasonable target for the future, since it better reflects the actual complexity of native human skin and has the potential to improve dermal development and epidermal stratification.[89,90]

From a small (4–$5\,cm^2$) skin biopsy, we could theoretically have generate approximately $180\,cm^2$ (five DESS). This takes less than $3\,h$ of work with the SkinFactory, but needs approximately 15–20 days to produce a mature graft ready for transplantation (Table 1). The manufacturing process without prevascularization would also allow a 90-fold expansion (i.e. production of $450\,cm^2$) within the same production time. The limiting factor seems to be the gain and expansion of an adequate number of endothelial cells, and we are working hard to accelerate this step. Our production time, even though seemingly long, is similar to the 4–5 weeks required for the skin analog developed by Boyce et al.[11] and significantly faster than the 8 weeks needed for the skin analog produced by Auger et al.[91] Nevertheless, it is our explicit goal to reduce production time, so that more acute cases could be treated in a clinical application.

Finally, the Fraunhofer Group has generated a robotic system (also called Skin Factory), in which all the bioengineered skin fabrication steps are carried out automatically.[92,93] The produced skin substitutes consisted of human fibroblasts embedded in a collagen scaffold and a stratified epidermis formed by human keratinocytes. No other cell types were included. The complete exclusion of human intervention increased the reproducibility and reduced the costs, but also reduced the adaptability of the system and did not accelerate significantly the process.[94] Therefore, we can imagine that the ultimate skin production system will probably amount to the collaboration of human and machine.

Conclusion

We show for the first time the engineering of an easy to handle, large-scale human pigmented and vascularized dermo-epidermal skin substitute and demonstrate its functionality in vivo. This achievement was accomplished by means of a new 3D bio-printer platform called SkinFactory, which includes modules for collagen hydrogel mixing and extrusion-based bioprinting, hydrogel plastic compression, and patterned inkjet delivery of various human skin derived cells. This study is as a proof of principle toward future clinical application of bio-printed vascularized autologous full skin dermo-epidermal skin substitutes as improved treatment option of burn victims and patients with severe skin lesions.

Authors' note

Andreas Scheidegger reports a relationship with RegenHU that includes: employment. Sandro Figi reports a relationship with RegenHU that includes: employment.

Data availability statement

The raw/processed data required to reproduce these findings cannot be shared at this time as the data also forms part of an ongoing study and due to legal or ethical reasons.

Declaration of conflicting interests

The author(s) declared the following potential conflicts of interest with respect to the research, authorship, and/or publication of

ORCID iD

Luca Pontiggia (iD) https://orcid.org/0000-0002-5553-8997

Supplemental material

Supplemental material for this article is available online.

References

1. Jeschke MG, Finnerty CC, Shahrokhi S, et al. Wound coverage technologies in burn care: novel techniques. *J Burn Care Res* 2013; 34(6): 612–620.

2. Martínez-Santamaría L, Guerrero-Aspizua S and Del Río M. Skin bioengineering: preclinical and clinical applications. *Actas Dermosifiliogr* 2012; 103(1): 5–11.

3. Biedermann T, Boettcher-Haberzeth S and Reichmann E. Tissue engineering of skin for wound coverage. *European J Pediatr Surg* 2013; 23(5): 375–382.

4. Lamme EN, Van Leeuwen RTJ, Brandsma K, et al. Higher numbers of autologous fibroblasts in an artificial dermal substitute improve tissue regeneration and modulate scar tissue formation. *J Pathol* 2000; 190(5): 595–603.

5. Stojic M, López V, Montero A, et al. 3. Skin tissue engineering. In: García-Gareta E (ed.) *Biomaterials for skin repair and regeneration*. Sawston CA: Woodhead Publishing, 2019, pp.59–99.

6. Knoz M, Holoubek J, Lipový B, et al. Skin substitutes in reconstruction surgery: the present and future perspectives. *Acta Chir Plast* 2020; 62(1–2): 18–23.

7. Oualla-Bachiri W, Fernández-González A, Quiñones-Vico MI, et al. From grafts to human bioengineered vascularized skin substitutes. *Int J Mol Sci* 2020; 21(21): 8197.

8. Meana A, Iglesias J, Del Rio M, et al. Large surface of cultured human epithelium obtained on a dermal matrix based on live fibroblast-containing fibrin gels. *Burns* 1998; 24(7): 621–630.

9. Llames S, García E, García V, et al. Clinical results of an autologous engineered skin. *Cell Tissue Bank* 2006; 7(1): 47–53.

10. Llames SG, Del Rio M, Larcher F, et al. Human plasma as a dermal scaffold for the generation of a completely autologous bioengineered skin. *Transplantation* 2004; 77(3): 350–355.

11. Boyce ST, Simpson PS, Rieman MT, et al. Randomized, paired-site comparison of autologous engineered skin substitutes and split-thickness skin graft for closure of extensive, full-thickness burns. *J Burn Care Res* 2017; 38(2): 61–70.

12. Germain L, Larouche D, Nedelec B, et al. Autologous bilayered self-assembled skin substitutes (SASSs) as permanent grafts: a case series of 14 severely burned patients indicating clinical effectiveness. *Eur Cell Mater* 2018; 36:128–141.

13. Böttcher-Haberzeth S, Biedermann T and Reichmann E. Tissue engineering of skin. *Burns* 2010; 36(4): 450–460.

14. Montaño I, Schiestl C, Schneider J, et al. Formation of human capillaries in vitro: the engineering of prevascularized matrices. *Tissue Eng Part A* 2010; 16(1): 269–282.

15. Biedermann T, Pontiggia L, Böttcher-Haberzeth S, et al. Human eccrine sweat gland cells can reconstitute a stratified epidermis. *J Investig Dermatol* 2010; 130:1996–2009.

16. Braziulis E, Biedermann T, Hartmann-Fritsch F, et al. Skingineering I: engineering porcine dermo-epidermal skin analogues for autologous transplantation in a large animal model. *Pediatr Surg Int* 2011; 27(3): 241–247.

17. Pontiggia L, Klar A, Böttcher-Haberzeth S, et al. Optimizing in vitro culture conditions leads to a significantly shorter production time of human dermo-epidermal skin substitutes. *Pediatr Surg Int* 2013; 29(3): 249–256.

18. Böttcher-Haberzeth S, Klar AS, Biedermann T, et al. Trooping the color": restoring the original donor skin color by addition of melanocytes to bioengineered skin analogs. *Pediatr Surg Int* 2013; 29(3): 239–247.

19. Biedermann T, Klar AS, Böttcher-Haberzeth S, et al. Tissue-engineered dermo-epidermal skin analogs exhibit de novo formation of a near natural neurovascular link 10 weeks after transplantation. *Pediatr Surg Int* 2014; 30(2): 165–172.

20. Klar AS, Güven S, Biedermann T, et al. Tissue-engineered dermo-epidermal skin grafts prevascularized with adipose-derived cells. *Biomaterials* 2014; 35(19): 5065–5078.

21. Böttcher-Haberzeth S, Biedermann T, Klar AS, et al. Characterization of pigmented dermo-epidermal skin substitutes in a long-termin vivoassay. *Exp Dermatol* 2015; 24(1): 16–21.

22. Meuli M, Hartmann-Fritsch F, Hüging M, et al. A cultured autologous dermo-epidermal skin substitute for full-thickness skin defects: A phase I, open, prospective clinical trial in children. *Plast Reconstr Surg* 2019; 144(1): 188–198.

23. Gómez C, Galán JM, Torrero V, et al. Use of an autologous bioengineered composite skin in extensive burns: clinical and functional outcomes: a multicentric study. *Burns* 2011; 37(4): 580–589.

24. Swope VB, Supp AP and Boyce ST. Regulation of cutaneous pigmentation by titration of human melanocytes in cultured skin substitutes grafted to athymic mice. *Wound Repair Regen* 2002; 10(6): 378–386.

25. Masnari O, Landolt MA, Roessler J, et al. Self- and parent-perceived stigmatisation in children and adolescents with congenital or acquired facial differences. *J Plast Reconstr Aesthet Surg* 2012; 65(12): 1664–1670.

26. Masnari O, Neuhaus K, Aegerter T, et al. Predictors of health-related quality of life and psychological adjustment in children and adolescents with congenital melanocytic nevi: analysis of parent reports. *J Pediatr Psychol* 2019; 44(6): 714–725.

27. Supp DM, Hahn JM, Lloyd CM, et al. Light or dark pigmentation of engineered skin substitutes containing melanocytes protects against ultraviolet light-induced DNA damage in vivo. *J Burn Care Res* 2020; 41(4): 751–760.

28. Biedermann T, Böttcher-Haberzeth S, Klar AS, et al. The influence of stromal cells on the pigmentation of tissue-engineered dermo-epidermal skin grafts. *Tissue Eng Part A* 2015; 21(5–6): 960–969.

29. Miyazaki H, Tsunoi Y, Akagi T, et al. A novel strategy to engineer pre-vascularized 3-dimensional skin substitutes to achieve efficient, functional engraftment. *Sci Rep* 2019; 9(1): 7797.

30. Marino D, Luginbühl J, Scola S, et al. Bioengineering dermo-epidermal skin grafts with blood and lymphatic capillaries. *Sci Transl Med* 2014; 6(221): 221ra14.

31. Braziulis E, Diezi M, Biedermann T, et al. Modified plastic compression of collagen hydrogels provides an ideal matrix for clinically applicable skin substitutes. *Tissue Eng Part C Methods* 2012; 18(6): 464–474.

32. Bishop ES, Mostafa S, Pakvasa M, et al. 3-D bioprinting technologies in tissue engineering and regenerative medicine: Current and future trends. *Genes Dis* 2017; 4(4): 185–195.

33. Roseti L, Cavallo C, Desando G, et al. Three-dimensional bioprinting of cartilage by the use of stem cells: A strategy to improve regeneration. *Materials* 2018; 11(9): 1749.

34. Ishack S and Lipner SR. A review of 3-dimensional skin bioprinting techniques: applications, approaches, and trends. *Dermatol Surg* 2020; 46(12): 1500–1505.

35. Ozbolat IT and Hospodiuk M. Current advances and future perspectives in extrusion-based bioprinting. *Biomaterials* 2016; 76:321–343.

36. Li X, Liu B, Pei B, et al. Inkjet bioprinting of Biomaterials. *Chem Rev* 2020; 120(19): 10793–10833.

37. Ovsianikov A, Gruene M, Pflaum M, et al. Laser printing of cells into 3D scaffolds. *Biofabrication* 2010; 2(1): 014104.

38. Lee V, Singh G, Trasatti JP, et al. Design and fabrication of human skin by three-dimensional bioprinting. *Tissue Eng Part C Methods* 2014; 20(6): 473–484.

39. Kim BS, Lee JS, Gao G, et al. Direct 3D cell-printing of human skin with functional transwell system. *Biofabrication* 2017; 9(2): 025034.

40. Kim BS, Kwon YW, Kong JS, et al. 3D cell printing of in vitro stabilized skin model and in vivo pre-vascularized skin patch using tissue-specific extracellular matrix bioink: A step towards advanced skin tissue engineering. *Biomaterials* 2018; 168:38–53.

41. Pontiggia L, Biedermann T, Meuli M, et al. Markers to evaluate the quality and self-renewing potential of engineered human skin substitutes in vitro and after transplantation. *J Investig Dermatol* 2009; 129(2): 480–490.

42. Santiago-Walker A, Li L, Haass NK, et al. Melanocytes: from morphology to application. *Skin Pharmacol Physiol* 2009; 22(2): 114–121.

43. Pensalfini M, Ehret AE, Stüdeli S, et al. Factors affecting the mechanical behavior of collagen hydrogels for skin tissue engineering. *J Mech Behav Biomed Mater* 2017; 69:85–97.

44. Michalczyk T, Biedermann T, Böttcher-Haberzeth S, et al. UVB exposure of a humanized skin model reveals unexpected dynamic of keratinocyte proliferation and Wnt inhibitor balancing. *J Tissue Eng Regen Med* 2018; 12(2): 505–515.

45. Schneider J, Biedermann T, Widmer D, et al. Matriderm versus Integra: a comparative experimental study. *Burns* 2009; 35(1): 51–57.

46. Gerdes J, Lemke H, Baisch H, et al. Cell cycle analysis of a cell proliferation-associated human nuclear antigen defined by the monoclonal antibody Ki-67. *J Immunol* 1984; 133(4): 1710–1715.

47. Fisch P, Holub M and Zenobi-Wong M. Improved accuracy and precision of bioprinting through progressive cavity pump-controlled extrusion. *Biofabrication* 2021; 13: 015012.

48. Lee M, Bae K, Levinson C, et al. Nanocomposite bioink exploits dynamic covalent bonds between nanoparticles and polysaccharides for precision bioprinting. *Biofabrication* 2020; 12(2): 025025.

49. Müller M, Fisch P, Molnar M, et al. Development and thorough characterization of the processing steps of an ink for 3D printing for bone tissue engineering. *Mater Sci Eng C Mater Biol Appl* 2020; 108:110510.

50. Müller M, Öztürk E, Arlov Ø, et al. Alginate sulfate-nanocellulose bioinks for cartilage bioprinting applications. *Ann Biomed Eng* 2017; 45(1): 210–223.

51. Ng WL, Qi JTZ, Yeong WY, et al. Proof-of-concept: 3D bioprinting of pigmented human skin constructs. *Biofabrication* 2018; 10(2): 025005.

52. Shi P, Tan YSE, Yeong WY, et al. A bilayer photoreceptor-retinal tissue model with gradient cell density design: A study of microvalve-based bioprinting. *J Tissue Eng Regen Med* 2018; 12(5): 1297–1306.

53. Cubo N, Garcia M, Del Cañizo JF, et al. 3D bioprinting of functional human skin: production and in vivo analysis. *Biofabrication* 2017; 9(1): 015006.

54. Jorgensen AM, Varkey M, Gorkun A, et al. Bioprinted skin recapitulates normal collagen remodeling in full-thickness wounds. *Tissue Eng Part A* 2020; 26(9–10): 512–526.

55. Quílez C, de Aranda Izuzquiza G, García M, et al. Bioprinting for Skin. In: Crook JM (ed.) *3D bioprinting: Principles and Protocols*. New York, NY: Springer US, 2020, pp.217–228.

56. Steinberg BM, Smith K, Colozzo M, et al. Establishment and transformation diminish the ability of fibroblasts to contract a native collagen gel. *J Cell Biol* 1980; 87(1): 304–308.

57. Zhu YK, Umino T, Liu XD, et al. Contraction of fibroblast-containing collagen gels: initial collagen concentration regulates the degree of contraction and cell survival. *In Vitro Cell Dev Biol Anim* 2001; 37(1): 10–16.

58. Harriger MD, Supp AP, Warden GD, et al. Glutaraldehyde crosslinking of collagen substrates inhibits degradation in skin substitutes grafted to athymic mice. *J Biomed Mater Res* 1997; 35(2): 137–145.

59. Powell HM and Boyce ST. EDC cross-linking improves skin substitute strength and stability. *Biomaterials* 2006; 27(34): 5821–5827.

60. Rimann M, Bono E, Annaheim H, et al. Standardized 3D bioprinting of soft tissue models with human primary cells. *J Lab Autom* 2016; 21(4): 496–509.

61. Mogoşanu GD and Grumezescu AM. Natural and synthetic polymers for wounds and burns dressing. *Int J Pharm* 2014; 463(2): 127–136.

62. Brown RA, Wiseman M, Chuo CB, et al. Ultrarapid engineering of biomimetic materials and tissues: fabrication of nano- and microstructures by plastic compression. *Adv Funct Mater* 2005; 15:1762–1770.

63. Baltazar T, Merola J, Catarino C, et al. Three dimensional bioprinting of a vascularized and perfusable skin graft using human keratinocytes, fibroblasts, pericytes, and endothelial cells. *Tissue Eng Part A* 2020; 26(5–6): 227–238.

64. Min D, Lee W, Bae IH, et al. Bioprinting of biomimetic skin containing melanocytes. *Exp Dermatol* 2018; 27(5): 453–459.

65. Young DM, Greulich KM and Weier HG. Species-specific in situ hybridization with fluorochrome-labeled DNA probes to study vascularization of human skin grafts on athymic mice. *J Burn Care Rehabil* 1996; 17(4): 305–310.

66. Mazio C, Casale C, Imparato G, et al. Pre-vascularized dermis model for fast and functional anastomosis with host vasculature. *Biomaterials* 2019; 192:159–170.

67. Richards D, Jia J, Yost M, et al. 3D bioprinting for vascularized tissue fabrication. *Ann Biomed Eng* 2017; 45(1): 132–147.

68. Kolesky DB, Truby RL, Gladman AS, et al. 3D bioprinting of vascularized, heterogeneous cell-laden tissue constructs. *Adv Mater* 2014; 26(19): 3124–3130.

69. Baranski JD, Chaturvedi RR, Stevens KR, et al. Geometric control of vascular networks to enhance engineered tissue integration and function. *Proc Natl Acad Sci USA* 2013; 110(19): 7586–7591.

70. Wu PK and Ringeisen BR. Development of human umbilical vein endothelial cell (HUVEC) and human umbilical vein smooth muscle cell (HUVSMC) branch/stem structures on hydrogel layers via biological laser printing (BioLP). *Biofabrication* 2010; 2(1): 014111.

71. Yanez M, Rincon J, Dones A, et al. In vivo assessment of printed microvasculature in a bilayer skin graft to treat full-thickness wounds. *Tissue Eng Part A* 2015; 21(1–2): 224–233.

72. Morgan JT, Shirazi J, Comber EM, et al. Fabrication of centimeter-scale and geometrically arbitrary vascular networks using in vitro self-assembly. *Biomaterials* 2019; 189:37–47.

73. Black AF, Berthod F, L'Heureux N, et al. In vitro reconstruction of a human capillary-like network in a tissue-engineered skin equivalent. *FASEB J* 1998; 12(13): 1331–1340.

74. Huyan Y, Lian Q, Zhao T, et al. Pilot Study of the biological properties and vascularization of 3D printed bilayer skin grafts. *Int J Bioprinting* 2020; 6(1): 246.

75. Shahin H, Elmasry M, Steinvall I, et al. Vascularization is the next challenge for skin tissue engineering as a solution for burn management. *Burns Trauma* 2020; 8:tkaa022.

76. Lee VK, Lanzi AM, Haygan N, et al. Generation of multiscale Vascular Network system within 3D hydrogel using 3D Bio-Printing technology. *Cell Mol Bioeng* 2014; 7(3): 460–472.

77. Zhou F, Hong Y, Liang R, et al. Rapid printing of bio-inspired 3D tissue constructs for skin regeneration. *Biomaterials* 2020; 258:120287.

78. Barros NR, Kim HJ, Gouidie MJ, et al. Biofabrication of endothelial cell, dermal fibroblast, and multilayered keratinocyte layers for skin tissue engineering. *Biofabrication* 2021; 13: 035030.

79. Liu X, Michael S, Bharti K, et al. A biofabricated vascularized skin model of atopic dermatitis for preclinical studies. *Biofabrication* 2020; 12(3): 035002.

80. Schechner JS, Crane SK, Wang F, et al. Engraftment of a vascularized human skin equivalent. *FASEB J* 2003; 17(15): 2250–2256.

81. Melero-Martin JM, Khan ZA, Picard A, et al. In vivo vasculogenic potential of human blood-derived endothelial progenitor cells. *Blood* 2007; 109(11): 4761–4768.

82. Lawlor KT and Kaur P. Dermal contributions to human interfollicular epidermal architecture and self-renewal. *Int J Mol Sci* 2015; 16(12): 28098–28107.

83. Michel M, Török N, Godbout MJ, et al. Keratin 19 as a biochemical marker of skin stem cells in vivo and in vitro: keratin 19 expressing cells are differentially localized in function of anatomic sites, and their number varies with donor age and culture stage. *J Cell Sci* 1996; 109(Pt 5): 1017–1028.

84. Webb A, Li A and Kaur P. Location and phenotype of human adult keratinocyte stem cells of the skin. *Differentiation* 2004; 72(8): 387–395.

85. Ghazizadeh S and Taichman LB. Organization of stem cells and their progeny in human epidermis. *J Investig Dermatol* 2005; 124(2): 367–372.

86. Mobasseri SA, Zijl S, Salameti V, et al. Patterning of human epidermal stem cells on undulating elastomer substrates reflects differences in cell stiffness. *Acta Biomater* 2019; 87:256–264.

87. Asencio IO, Mittar S, Sherborne C, et al. A methodology for the production of microfabricated electrospun membranes for the creation of new skin regeneration models. *J Tissue Eng* 2018; 9:2041731418799851.

88. Malara MM, Blackstone BN, Baumann ME, et al. Cultured epithelial autograft combined with micropatterned dermal template forms rete ridges in vivo. *Tissue Eng Part A* 2020; 26(21-22): 1138–1146.

89. Kober J, Gugerell A, Schmid M, et al. Generation of a fibrin based three-layered skin substitute. *Biomed Res Int* 2015; 2015(2015): 170427.

90. Kim BS, Gao G, Kim JY, et al. 3D cell printing of perfusable vascularized human skin equivalent composed of epidermis, dermis, and hypodermis for better structural recapitulation of native skin. *Adv Healthc Mater* 2019; 8(7): e1801019.

91. Auger FA, López Valle CA, Guignard R, et al. Skin equivalent produced with human collagen. *In Vitro Cell Dev Biol Anim* 1995; 31(6): 432–439.

92. Festo SE & Co. KG. The skin factory - Automated tissue engineering, 2016.

93. Walles H and Pickert D. The skin factory, 2011.

94. Sarkiri M, Fox SC, Fratila-Apachitei LE, et al. Bioengineered skin intended for skin disease modeling. Int J Mol Sci 2019;20(6): 1407.